

Article

Tunnel Boring Machine Performance Prediction Using Supervised Learning Method and Swarm Intelligence Algorithm

Zhi Yu ¹, Chuanqi Li ^{2,*} and Jian Zhou ³¹ Zijin School of Geology and Mining, Fuzhou University, Fuzhou 350116, China; zhi.yu@fzu.edu.cn² Laboratory 3SR, CNRS UMR 5521, Grenoble Alpes University, 38000 Grenoble, France³ School of Resources and Safety Engineering, Central South University, Changsha 410083, China; j.zhou@csu.edu.cn

* Correspondence: chuanqi.li@univ-grenoble-alpes.fr

Abstract: This study employs a supervised learning method to predict the tunnel boring machine (TBM) penetration rate (PR) with high accuracy. To this end, the extreme gradient boosting (XGBoost) model is optimized based on two swarm intelligence algorithms, i.e., the sparrow search algorithm (SSA) and the whale optimization algorithm (WOA). Three other machine learning models, including random forest (RF), support vector machine (SVM), and artificial neural network (ANN) models, are also developed as the drawback. A database created in Shenzhen (China), comprising 503 entries and featuring 10 input variables and 1 output variable, was utilized to train and test the prediction models. The model development results indicate that the use of SSA and WOA has the potential to improve the XGBoost model performance in predicting the TBM performance. The performance evaluation results show that the proposed WOA-XGBoost model has achieved the most satisfactory performance by resulting in the most reliable prediction accuracy of the four performance indices. This research serves as a compelling illustration of how combined approaches, such as supervised learning methods and swarm intelligence algorithms, can enhance TBM prediction performance and can provide a reference when solving other related engineering problems.

Citation: Yu, Z.; Li, C.; Zhou, J. Tunnel Boring Machine Performance Prediction Using Supervised Learning Method and Swarm Intelligence Algorithm. *Mathematics* **2023**, *11*, 4237. <https://doi.org/10.3390/math11204237>

Academic Editor: Ioannis G. Tsoulos

Received: 23 September 2023

Revised: 8 October 2023

Accepted: 9 October 2023

Published: 10 October 2023



Copyright: © 2023 by the authors. Licensee MDPI, Basel, Switzerland. This article is an open access article distributed under the terms and conditions of the Creative Commons Attribution (CC BY) license (<https://creativecommons.org/licenses/by/4.0/>).

Keywords: tunnel boring machine; penetration rate; extreme gradient boosting; swarm intelligence algorithm

MSC: 68T20

1. Introduction

With the development of the economy and society, urban ground space can no longer adequately accommodate the growing demands of transportation. Consequently, there is a need to expand transportation systems below ground. In response, an increasing number of cities, particularly major international urban centers, have embarked on the construction of underground metro systems. Meanwhile, considering the characteristics of a high excavation efficiency, a low construction cost, and small negative environmental impacts [1,2], the Tunnel Boring Machine (TBM) technique has gained widespread utilization in metro construction. However, its performance is significantly influenced by machine parameters, surface topography, and geological conditions, thereby introducing substantial project construction instability. To provide reasonable support for engineering period planning, controlling engineering costs, and minimizing common risk probability [3,4], the accurate prediction of TBM performance has become a pressing and consequential engineering challenge.

In the existing literature, three parameters, namely, the penetration rate (PR), advance rate (AR), and utilization index (UI), have been employed for assessing the TBM performance [5–8]. Among them, the PR represents the ratio of the excavation distance to the operation time, and it has found extensive application in published studies [9]. Over time, numerous empirical and theoretical models have been applied to evaluate the penetration rate of TBMs. For instance, the Colorado School of Mines (CSM) model [10], established through laboratory tests and rock-breaking mechanisms, has gained wide acceptance. Similarly, the Norwegian University of Science and Technology (UTNU) model [11], which considers the interaction between hob and rock mass, enjoys popularity. Nonetheless, these models exhibit variability in prediction performance due to their limited consideration of variables [12]. Moreover, the presence of constants in these models significantly impacts their applicability [13].

In recent years, artificial intelligence (AI) technology has been rapidly developed, as well as its ability to establish a robust relationship between input and output variables. This technology has been demonstrated through the successful resolution of various engineering challenges in the fields of medicine [14], agriculture [15], machinery [16], and mining [17–20]. Unlike the empirical and the theoretical models, the AI technology represented by the machine learning (ML) models does not have limitations on the number of input variables and does not rely on constants [13,21], addressing some of the drawbacks associated with traditional models. Moreover, due to their complex model structures and high computational capabilities, ML models can solve nonlinear problems more effectively than most traditional models. The literature shows that the ML technique is increasingly applied to predict the PR of TBM. For instance, Armaghani et al. [22] utilized two optimized artificial neural networks (ANN) models to predict the PR based on a database collected from the Pahang–Selangor raw water transfer (PSRWT) tunnel in Malaysia. Alvarez Grima et al. [23] employed an adaptive neuro-fuzzy inference system (ANFIS) model to predict the PR values of TBM. Mahdevari et al. [24] established a nonlinear relationship between machine parameters and PR using a support vector regression (SVR) model. Koopialipoor et al. [25] applied a deep neural network (DNN) to analyze the PR of TBM based on the Pahang–Selangor raw water transfer tunnel database. Furthermore, more applications of ML techniques in investigating the TBM performance can be found in the studies of Xu et al. [26], Zhou et al. [27], Torabi et al. [5], Wang et al. [28], and Agrawal et al. [29]. Although numerous studies have explored the application of ML techniques in assessing the TBM performance of PR, limited attention has been given to investigating the suitability of the XGBoost method, particularly the optimized XGBoost model, for predicting the PR of TBM. Meanwhile, there is a scarcity of research on TBM performance prediction in complex geological conditions characterized by composite strata and a relatively high proportion of boulders. Furthermore, the advancement in swarm optimization algorithms offers an alternative approach for exploring the optimal hyperparameter combination in a supervised learning model. However, the integration of the swarm optimization algorithm with the XGBoost model is relatively uncommon. Therefore, the present study aims to introduce a hybrid prediction approach for predicting the PR of TBM by combining a supervised learning method with two popular swarm intelligence algorithms called the sparrow search algorithm (SSA) and the whale optimization algorithm (WOA). Here, two novel proposed hybrid XGBoost models, including SSA-XGBoost and WOA-XGBoost models, are proposed, and the XGBoost, random forest (RF), support vector machine (SVM), and ANN models are also prepared as the benchmark using the same input and output variables. In the subsequent sections, first, the backgrounds of the XGBoost, SSA, and WOA are given. Then, the procedure of combining XGBoost and swarm intelligence algorithm is introduced. After that, the application of these models in predicting TBM performance using the Shenzhen Metro Line 10 database is described. Eventually, a sensitivity analysis is conducted to identify the most crucial parameters for predicting the PR of TBM.

2. Related Work

In this section, the related work of using the ML method to predict TBM PR is reviewed and presented. In this presented study, three kinds of input variables, including machine, composite stratum, and boulder parameters, are considered and utilized as the input variables, and the PR is the output variable. Consequently, the related works are shown in Table 1. As shown, Yagize et al. [30] used an ANN to establish a prediction model for estimating TBM performance, and 151 datasets collected from Queens Tunnels in the City of New York, USA were analyzed. Rock material, TBM, and rock mass properties were used as the input variables, while PR was the output variable. Their analysis revealed highly accurate performance estimations. Xu et al. [26] found that KNN has the highest prediction precision based on a database collected from the PSRWT project in Malaysia. Shan et al. [8] applied a long short term memory (LSTM) model to evaluate the TBM performance of metros located in the cities of Changsha to Zhengzhou, China, and the obtained results show that the performance of Recurrent Neural Networks (RNN) surpassed that of LSTM. In addition, for the hybrid model, Armaghani et al. [22] introduced an ANN optimized by imperialism competitive algorithm (ICA) to predict the TBM PR in the PSRWT project. They found that the ICA-ANN model had a determination coefficient of 0.912 for testing data. It was also found that the performance of ICA-ANN was much better than that of ANN model. By proposing 6 optimized XGB-based models based on 1286 datasets, Zhou et al. [27] identified the particle swarm optimization (PSO)-XGBoost model, which yielded an impressive R-squared (R^2) value of 0.951, as a highly accurate, powerful, and practical approach for TBM performance prediction. Similar research endeavors can be observed using stacking framework optimized by whale optimization algorithm (Stacking-WOA) and improved sparrow search algorithm-gradient boosting regression tree technique (ISSA-GBRT) in the studies conducted by Song et al. [31] and Yang et al. [32], respectively.

Table 1. Related works on TBM PR prediction using ML method.

Study	ML Model	Input Variables	Output Variable	Samples
Yagiz et al. [30]	ANN	Rock material properties TBM parameters	PR	151
Xu et al. [26]	KNN	Machine characteristics Rock mass properties Rock material properties	PR	209
Shan et al. [8]	RNN	Machine characteristics	PR	550
Armaghani et al. [22]	ICA-ANN	Machine characteristics Rock mass properties Rock material properties	PR	1286
Zhou et al. [27]	PSO-XGBoost	Machine characteristics Rock mass properties Rock material properties	PR	1286
Song et al. [31]	Stacking-WOA	Rock material properties Machine characteristics	PR	591
Yang et al. [32]	ISSA-GBRT	Machine characteristics Composite stratum parameters Bolder parameters	PR	308

3. Methodology

3.1. Extreme Gradient Boosting (XGBoost)

XGBoost, initially introduced by Chen and He [33], is a robust decision tree algorithm founded on the gradient boosting tree method [34]. This algorithm excels in the efficient construction of boosted trees and can be effectively employed to address both

classification and regression tasks. In the development of the XGBoost model, the residual is strategically employed to enhance the model performance by optimizing the loss function, while a regularization term is incorporated to mitigate the risk of overfitting [35].

In general, an objective function $Obj(x)$ for the XGBoost model can be described as follows:

$$Obj(x) = g(x) + k(x) \tag{1}$$

where x is the input variable. $f(x)$ and $g(x)$ are the residual and regular term, respectively.

The prediction results (\hat{y}) of the i th sample after t th iteration can be defined as follows:

$$\begin{aligned} \hat{y}_i^0 &= f_0(x_i) = 0 \\ \hat{y}_i^1 &= f_1(x_i) = f_0(x_i) + f_1(x_i) = \hat{y}_i^0 + f_1(x_i) \\ \hat{y}_i^2 &= f_2(x_i) = f_1(x_i) + f_2(x_i) = \hat{y}_i^1 + f_2(x_i) \\ &\dots \\ \hat{y}_i^t &= \sum_{k=1}^t f_k(x_i) = f_{t-1}(x_i) + f_t(x_i) = \hat{y}_i^{t-1} + f_t(x_i) \end{aligned} \tag{2}$$

Meanwhile, the regular term can be defined as follows:

$$g(x) = \gamma T + 0.5\lambda \sum_{j=1}^T \omega^2 \tag{3}$$

where T is the number of leaves, and w is the vector of scores on leaves. Additionally, γ and λ represent constants employed to regulate the tree's complexity.

Therefore, the object function $Obj(x)$ can be transformed into the following:

$$Obj(x) = \sum_{i=1}^n g\left(y_i, \hat{y}_i^{t-1} + f_t(x_i)\right) + \gamma T + 0.5\lambda \sum_{j=1}^T \omega^2 \tag{4}$$

3.2. Sparrow Search Algorithm

Sparrows are social birds found worldwide and are distinguished by their high intelligence and strong memory in comparison to other avian species. Their social behavior categorizes sparrows into producers and scroungers, with sparrows frequently transitioning between these roles to locate superior food sources [36]. The individual's role within the group is primarily dictated by their energy reserves, which means that sparrows with lower energy reserves are more likely to adopt the scrounger role. Thus, Xue and Shen [37] introduced a swarm intelligence algorithm known as the Sparrow Search Algorithm (SSA) to solve the optimization problem.

In the SSA, the producers are responsible for searching food and providing foraging areas or directions for all scroungers, so producers have a broad search range. In each search iteration, the producer's position can be updated as follows:

$$X_{i,j}^{t+1} = \begin{cases} X_{i,j}^t \cdot \exp\left(\frac{-i}{\alpha \cdot iter_{\max}}\right) & \text{if } R_2 < ST \\ X_{i,j}^t + Q \cdot L & \text{if } R_2 \geq ST \end{cases} \tag{5}$$

where t and $iter_{\max}$ are the current iterations and the largest number of iterations, respectively. $X_{i,j}^t$ means the value of the j th dimension of the i th sparrow at the t th iteration. α is a random number. R_2 and ST are the alarm value and the safety threshold, respectively.

A sparrow will move to a broad search range when $R_2 < ST$ and will fly back to the safe area in other cases.

The position of the scrounger can be described as follows:

$$X_{i,j}^{t+1} = \begin{cases} Q \cdot \exp\left(\frac{X_{worst}^t - X_{i,j}^t}{i^2}\right) & \text{if } i > \frac{n}{2} \\ X_p^{t+1} + |X_{i,j}^t - X_p^{t+1}| \cdot A^+ \cdot L & \text{otherwise} \end{cases} \quad (6)$$

where X_p is the optimal position of the producer, and X_{worst} means the current global worst position of the scrounger.

When a sparrow is aware of danger, these sparrows will fly back to the safe area, and this behavior can be expressed using the following mathematical equation:

$$X_{i,j}^{t+1} = \begin{cases} X_{best}^t + \beta \cdot |X_{i,j}^t - X_{best}^t| & \text{if } f_i > f_g \\ X_{i,j}^t + K \cdot \left(\frac{|X_{i,j}^t - X_{worst}^t|}{(f_i - f_w) + \varepsilon}\right) & \text{if } f_i = f_g \end{cases} \quad (7)$$

where X_{best} is the current global optimal position. β and k are the step size control parameter and a random number, respectively. Meanwhile, f_i, f_g , and f_w are the fitness values of the current sparrow and the current global best and worst fitness values, respectively.

Using the above-presented mathematical formulas, the updated sparrow location can be achieved, and the best solution for an engineering problem can be found with an initialization sparrow population.

3.3. Whale Optimization Algorithm

As a nature-inspired population-based optimization algorithm, the WOA algorithm is inspired by the bubble-net feeding of humpback whales in the ocean [38]. WOA encompasses three key stages: encircling prey, bubble-net attacking, and searching around the best prey.

Before attacking, humpbacks enclose the fish and then try to find the optimum solution. In this stage, the mathematical formula of the position updating can be expressed as

$$X_{i+1} = X_i - A|CX_i^* - X_i| \quad (8)$$

where X_i, X_{i+1} , and X_i^* are the current individual position of whale, the individual position of whale after i th iteration, and the current optimal individual position, respectively. In addition, A and C are both coefficients.

In the bubble-net preying phase, two social behaviors, including shrink wrapping and spiral uprising, can be selected for the humpback. Generally, the selection probability between two cases is 0.5, and local optimization can be achieved through these processes. In this algorithm, the mathematical model is expressed as follows:

$$X_{i+1} = \begin{cases} X_i - A|CX_i^* - X_i| & p < 0.5 \\ |X_i^* - X_i|e^{bl} \cos(2\pi l) + X_i^* & p \geq 0.5 \end{cases} \quad (9)$$

where b is a constant defining the spiral shape, and l and p are both random numbers.

In the searching phase, a whale can explore the food source by adjusting the parameter A , and this hunting behavior can be represented as follows:

$$X_{i+1} = X_{rand} - A|CX_{rand} - X_i| \quad (10)$$

where X_{rand} is the randomly selected whale position.

3.4. Hybrid XGBoost Model

In an XGBoost model, some hyperparameters, such as the number of trees, learning rate, and minimum child weight, are typically determined using the trial-and-test method. In this case, finding the optimal combination of hyperparameters can often be challenging. Hence, many researchers have explored the use of meta-heuristic algorithms to assist in hyperparameter selection, and the effectiveness of this approach has been demonstrated. In this study, two swarm intelligence algorithms, including the sparrow search algorithm and the whale optimization algorithm, were applied to select the optimal hyperparameters of the XGBoost model for predicting the PR of TBM, as shown in Figure 1.

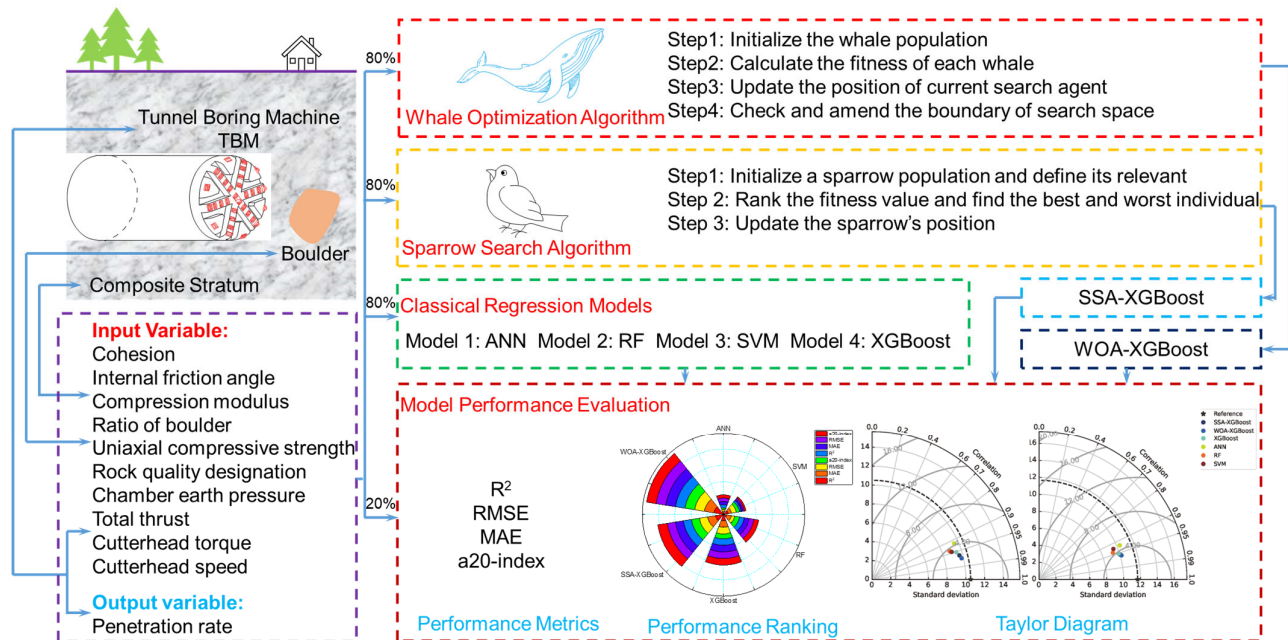


Figure 1. Procedure of using machine learning method to predict TBM performance.

As can be seen in the above picture, the procedure for establishing SSA-XGBoost and WOA-XGBoost models involves the following steps:

- (1) Collect the input and output variables based on engineering problems.
- (2) Scale the collected datasets into the same data range.
- (3) Divide the collected database into training and test datasets, with the training dataset used for training models and the test dataset used for assessing the prediction performance of the trained models.
- (4) Use the SSA and WOA to search the optimal hyperparameter combinations, incorporating validation methods like k-fold cross-validation to mitigate issues of underfitting and overfitting. In this study, 10-fold cross-validation is utilized. In the utilization of SSA in searching for the optimal hyperparameter combination, the best sparrow position is regarded as the optimal solution to the engineering problem. During each iteration, the discovered solution undergoes testing via the 10-fold cross-validation technique, and the resulting fitness value is employed to steer the exploration of optimal solutions within SSA. This process terminates once the predefined error threshold is attained. A similar procedure is observed in the application of WOA to optimize the XGBoost model.
- (5) Construct the optimal model for predicting the PR of TBM based on the identified hyperparameter combination.
- (6) Evaluate the prediction model's performance using various evaluation techniques such as the performance ranking or the Taylor diagrams.

3.5. Performance Evaluation

To evaluate the prediction performance, four performance indices, including coefficient of determination (R^2), mean absolute error (MAE), root-mean-squared error (RMSE), and a20-index, are employed and computed, as defined by the following formulas [39–45].

$$R^2 = 1 - \frac{\sum_{i=1}^n (PR_a - PR_p)^2}{\sum_{i=1}^n (PR_a - \overline{PR_a})^2} \quad (11)$$

$$MAE = \frac{1}{n} \sum_{i=1}^n |PR_a - PR_p| \quad (12)$$

$$RMSE = \sqrt{\frac{1}{n} (PR_a - PR_p)^2} \quad (13)$$

$$a20 - index = \frac{n_{20}}{n} \quad (14)$$

where PR_a , PR_p , and n represent the actual PR value, predicted PR value, and the number of samples, respectively. a20-index is defined as the count of datasets where the ratio of actual values to predicted values falls within the range of 0.8 to 1.2. Furthermore, an optimal prediction model is characterized by an R^2 value of 1, an a20-index of 1, an MAE value of 0, and an RMSE value of 0.

While this study employs four performance indices, it can be challenging to identify a prediction model that outperforms others across all performance indices for both training and test datasets. Therefore, comprehensive comparative methods are essential. In this study, a ranking method and a Taylor diagram approach are selected. In the ranking method, each performance index's computed values are ranked, and the prediction models are evaluated based on their total ranking values. A higher total ranking value indicates a superior prediction performance. For the Taylor diagram, it offers a comprehensive comparison of standard deviation, RMSE, and correlation coefficient. Each prediction model is represented by a colored point on the Taylor diagram, with an ideal model performance indicated by a black star. If the position of the prediction model is closer to the black star, it has a better performance than other models.

4. Engineering Validation

4.1. Materials

Shenzhen Metro Line 10 is part of the Shenzhen Metro system (see Figure 2a) and started operation on 18 August 2020. As shown in Figure 2b, this Metro Line starts from the Futian Port Station and ends at the Shuangyong Street Station, and the tunnel between the Beier Road Station and the Bantian North Road Station was constructed using a TBM. According to the geological survey results [9], this tunnel passes through the composite strata, including gravel cohesive soil, fully weathered granite, and sand-like strongly weathered granite and multiple boulder groups. Generally, the PR of TBM is influenced by the machine parameters and the geological conditions.

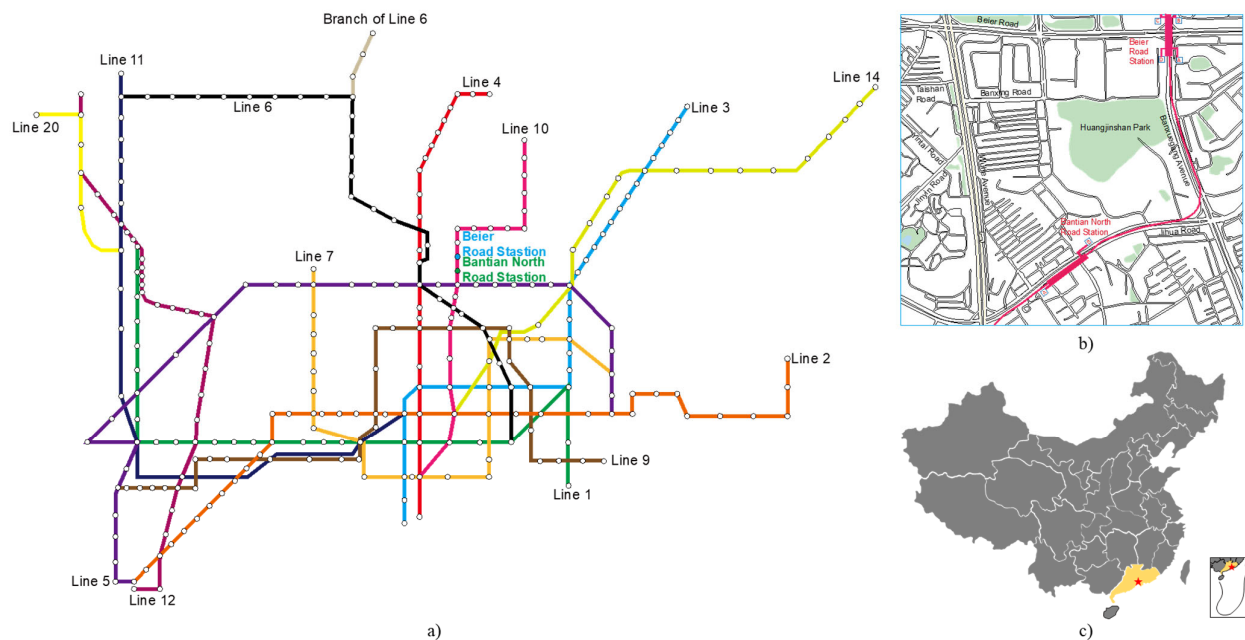


Figure 2. Shenzhen Metro Line 10. (a) Shenzhen Metro system. (b) A view of the study area. (c) Location of the metro in China.

In this study, 503 datasets (see Figure 3) provided by Yang et al. [9] were selected and used to develop a ML model. Among them, four machine parameters (chamber earth pressure (CEP), total thrust (TT), cutterhead torque (CT), and cutterhead speed (CS)), three composite stratum parameters (cohesion (c), internal friction angle (IFA), and compression modulus (CM)), and three boulder parameters (the ratio of boulder (RB), uniaxial compressive strength (UCS), and rock quality designation (RQD)) were selected as the input variables. Of these variables, the machine parameters were acquired from the TBM records. Data related to the composite stratum and boulder parameters were gathered through drilling and laboratory experiments. The ratio of boulders was determined utilizing the three-dimensional resistivity CT method. Meanwhile, the PR of TBM served as an output variable. The statistical distribution of the input and output variables is plotted in Figure 3.

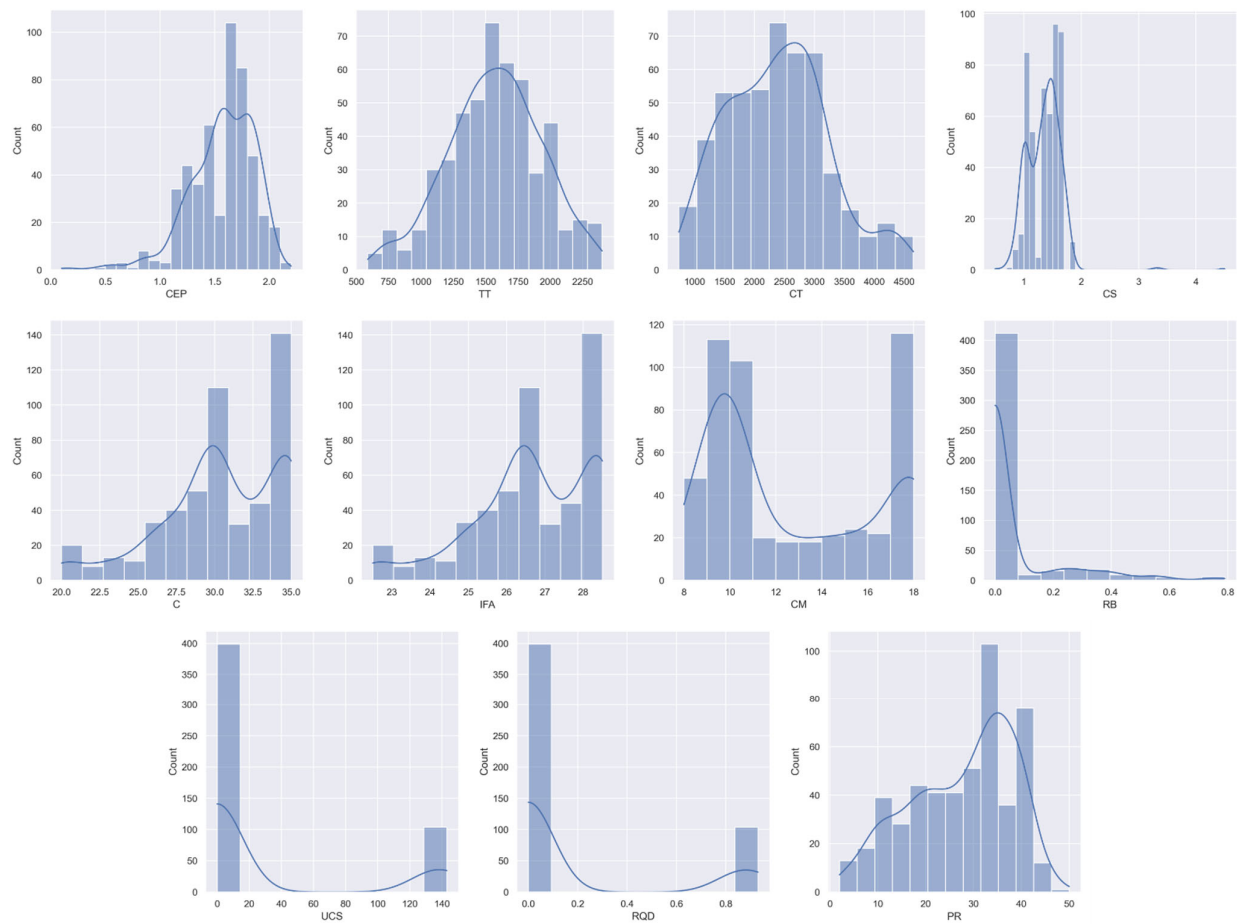


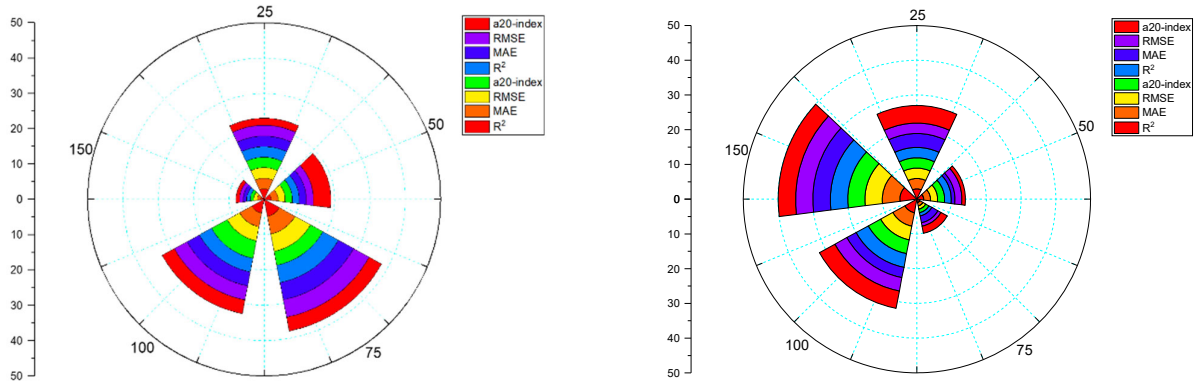
Figure 3. Parameter distribution of the input and output variables.

4.2. Performance Comparison

To validate the prediction performance of the proposed SSA-XGBoost model and WOA-XGBoost model, the collected TBM database was normalized into a range of 0 to 1, and then this database was divided into training and test datasets with a ratio of 80% to 20% [46,47]. Next, the XGBoost model was trained by SSA and WOA to search for the optimal hyperparameter combination. Meanwhile, a 10-fold cross-validation method was applied to guide the search process to avoid overfitting. In this process, a training dataset can be divided into 10 folds; 9 subsets are used to train the prediction model, and the remaining 1 is selected to evaluate the performance with the corresponding hyperparameter combination in the current iteration [48]. Meanwhile, the RMSE value calculated from the fitness function is used as the prediction error. In each iteration, the above calculation process will be repeated 10 times, and the average result of 10 fitness values will be used as the final performance of the current iteration.

For the SSA-XGBoost model, two parameters, including the swarm population and the maximum number of iterations, should be defined. Following the methodology outlined in the studies by Zhou et al. [49] and Faradonbeh et al. [50], a maximum of 100 iterations was set, and the swarm population values were varied across values of 25, 50, 75, 100, and 150. Table 2 and Figure 4a show the calculated performance metrics, and a ranking method provided by Zorlu et al. [51] is employed, respectively. After developing five optimal SSA-XGBoost models, the index values of the training and test datasets were ranked to comprehensively explain the model performance. Then, the best SSA-XGBoost model with a swarm population of 75 and a total ranking value of 38 was determined to

have a performance of R^2 of 0.93, MAE of 2.19, RMSE of 2.82, and an a20-index of 0.88 using the training datasets, as well as R^2 of 0.93, MAE of 2.19, RMSE of 2.82, and a20-index of 0.88 using the test datasets.



(a) SSA-XGBoost.

(b) WOA-XGBoost.

Figure 4. Comprehensive ranking comparison of two optimized XGBoost models with various swarm populations.

Table 2. The performance of optimizing XGBoost models with SSA.

Swarm Population	Training Dataset				Test Dataset				Total
	R^2	MAE	RMSE	a20-Index	R^2	MAE	RMSE	a20-Index	
25	0.92	2.39	3.05	0.86	0.90	2.80	3.68	0.80	-
50	0.91	2.43	3.13	0.85	0.89	2.89	3.78	0.83	-
75	0.93	2.19	2.82	0.88	0.90	2.70	3.60	0.81	-
100	0.93	2.24	2.86	0.89	0.90	2.75	3.64	0.81	-
150	0.90	2.62	3.34	0.84	0.89	2.98	3.88	0.79	-
25	3	3	3	3	3	3	3	2	23
50	2	2	2	2	2	2	2	5	19
75	5	5	5	4	5	5	5	4	38
100	4	4	4	5	4	4	4	4	33
150	1	1	1	1	1	1	1	1	8

In the case of WOA-XGBoost modeling with the same training and test datasets, five WOA-XGBoost models were developed, employing swarm populations of 25, 50, 75, 100, and 150. Based on the calculated performance metrics and comprehensive ranking, as shown in Table 3 and Figure 4b, the optimal swarm population, with a total ranking value of 40, can be determined to be 150. Additionally, the optimal WOA-XGBoost model exhibited the following performance metrics: R^2 of 0.95, MAE of 1.91, RMSE of 2.45, and an a20-index of 0.92 using the training dataset, and R^2 of 0.91, MAE of 2.62, RMSE of 3.41, and a20-index of 0.81 using the test dataset.

Table 3. The performance of optimizing XGBoost models with WOA.

Swarm Population	Training Dataset				Test Dataset				Total
	R^2	MAE	RMSE	a20-Index	R^2	MAE	RMSE	a20-Index	
25	0.93	2.24	2.87	0.88	0.91	2.67	3.55	0.81	-
50	0.91	2.52	3.22	0.86	0.89	2.87	3.79	0.79	-
75	0.90	2.54	3.24	0.85	0.89	2.87	3.80	0.80	-

100	0.93	2.21	2.84	0.89	0.91	2.68	3.54	0.81	-
150	0.95	1.91	2.45	0.92	0.91	2.62	3.41	0.81	-
25	3	3	3	3	3	4	3	5	27
50	2	2	2	2	2	1	2	1	14
75	1	1	1	1	1	2	1	2	10
100	4	4	4	4	4	3	4	5	32
150	5	5	5	5	5	5	5	5	40

In addition to the introduced SSA-XGBoost and WOA-XGBoost models, four conventional models, namely XGBoost, RF, SVM, and ANN, were also developed for the purpose of comparison. Similar to the process for determining the optimal SSA-XGBoost and WOA-XGBoost models, the performance indices of the XGBoost, RF, SVM, and ANN were computed and ranked. In this procedure, the trial-and-error method was employed to ascertain the hyperparameters for the RF, SVM, and ANN models. For the RF model, the hyperparameters to be determined included the number of trees and the number of variables used for each tree’s growth. In the case of the SVM model, the hyperparameters were the penalty factor (C) and gamma (g) in the RBF kernel. As for the ANN model, the sole hyperparameter was the number of nodes in the hidden layer. As depicted in Table 4 and Figure 5, these prediction models can be arranged in the following order based on their performance improvement: ANN, SVM, RF, XGBoost, SSA-XGBoost, and WOA-XGBoost.

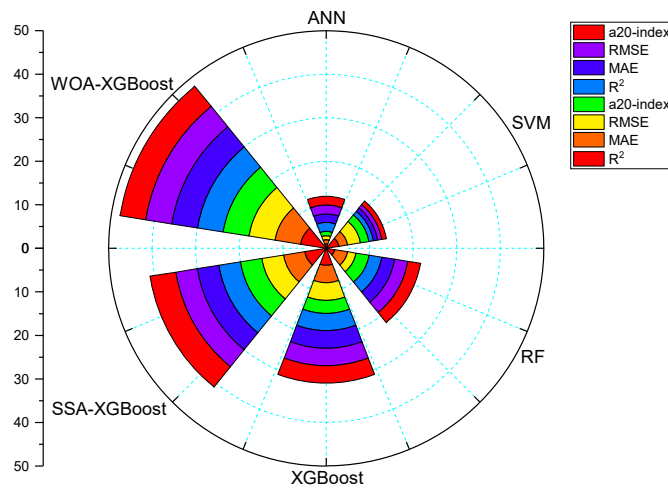


Figure 5. Comprehensive ranking comparison of various XGBoost prediction models.

Table 4. The performance of various TBM performance prediction models.

Swarm Pop- ulation	Training Dataset				Test Dataset				Total
	R ²	MAE	RMSE	a20- Index	R ²	MAE	RMSE	a20- Index	
XGBoost	0.90	2.56	3.26	0.85	0.89	2.85	3.78	0.80	-
RF	0.87	2.86	3.77	0.80	0.86	3.23	4.31	0.77	-
SVM	0.89	3.11	3.55	0.78	0.84	3.71	4.58	0.73	-
ANN	0.84	3.30	4.20	0.76	0.85	3.42	4.52	0.74	-
WOA- XGBoost	0.95	1.91	2.45	0.92	0.91	2.62	3.41	0.81	-
SSA- XGBoost	0.93	2.19	2.82	0.88	0.90	2.70	3.60	0.81	-
XGBoost	4	4	4	3	4	4	4	4	31
RF	2	3	2	3	3	3	3	3	22

SVM	3	2	3	2	1	1	1	1	14
ANN	1	1	1	1	2	2	2	2	12
WOA-XGBoost	6	6	6	6	6	6	6	6	48
SSA-XGBoost	5	5	5	5	5	5	5	6	41

Apart from the computation of performance indices and the presented ranking outcomes, the comparison of actual and predicted PR values of TBM is graphically illustrated in Figure 6. It is easy to find that the predicted results provided by the WOA-XGBoost model have the highest distribution frequency. Meanwhile, a greater number of data points signify that the predicted results are distributed within the range where the ratio of the predicted PR to the actual PR falls between 0.8 and 1.2. Consequently, the prediction performance of the WOA-XGBoost model is substantiated.

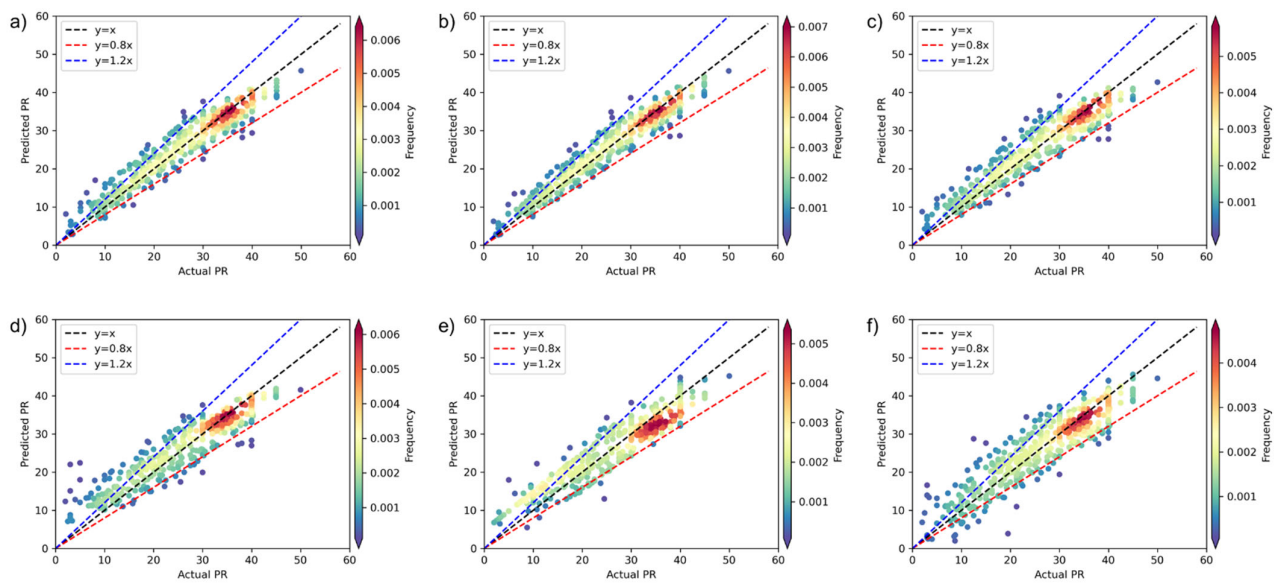


Figure 6. Correlation analysis of the actual and predicted TBM performance. (a) SSA-XGBoost. (b) WOA-XGBoost. (c) XGBoost. (d) RF. (e) SVM. (f) ANN.

To provide a comprehensive comparison of prediction performance, the Taylor diagram, originally proposed by Taylor [52], is employed and depicted in Figure 7. This diagram encompasses the calculation and presentation of the standard deviation, RMSE, and correlation coefficient of the PR prediction model. The model positioned closest to the reference point, denoted by a black star, signifies superior performance. As evident, the hybrid XGBoost model, particularly the WOA-XGBoost model, outperformed all other models.

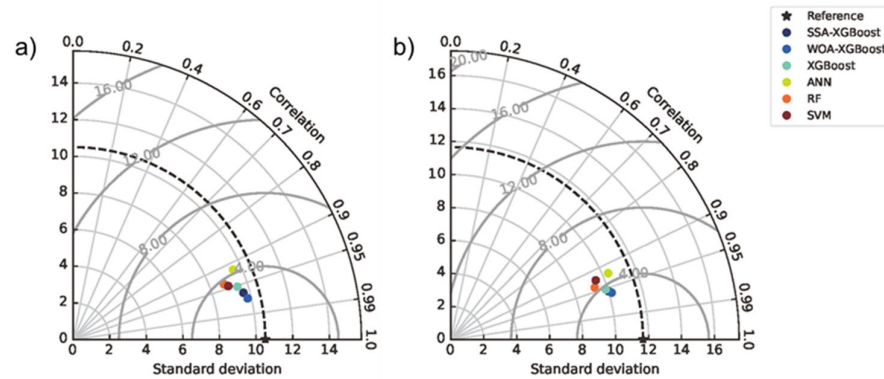


Figure 7. Taylor diagrams of the training and testing datasets. (a) Training datasets. (b) Testing datasets.

In summary, the WOA-XGBoost model demonstrated the best prediction performance for both training and test datasets, and it is highly recommended for TBM performance prediction. Meanwhile, the proposed WOA-XGBoost model had an R^2 of 0.95 and 0.91 for training and test datasets, which is better than the prediction model provided by Yang et al. [9].

4.3. Sensitivity Analysis

In addition to achieving accurate predictions of TBM performance, it is essential to address the challenge of effectively controlling and enhancing TBM performance. To fulfill this objective, a sensitivity analysis is crucial for assessing the sensitivity of each input variable and optimizing engineering design. In this context, the cosine amplitude method [53–55] was selected, and the relationship between the input variable X_i and the output variable \hat{X}_j can be computed using the following equation.

$$r_{ij} = \frac{\sum_{k=1}^n x_{ik} x_{jk}}{\sqrt{\sum_{k=1}^n x_{ik}^2} \times \sqrt{\sum_{k=1}^n x_{jk}^2}} \tag{15}$$

As shown in Figure 8, all the input variables can be ranked in descending order as follows: CS, CEP, TT, IFA, CT, C, CM, UCS, RQD, and PB. Notably, C, IFA, CM, RB, UCS, and RQD cannot be changed during the construction, leaving the machine parameters, particularly the cutterhead speed, as the sole potential avenue for enhancing TBM performance.

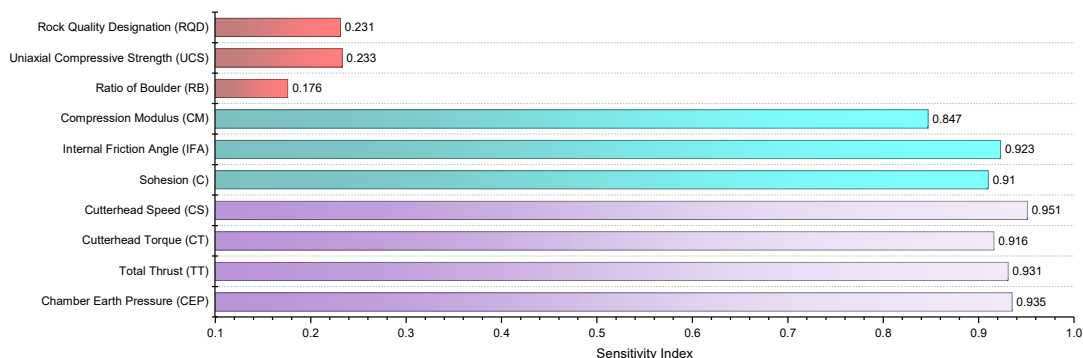


Figure 8. Sensitivity analysis of input variables on TBM performance. The red, blue, and purple bars represent boulder, composite stratum, and machine parameters, respectively.

5. Discussion

To facilitate engineering period planning, cost reduction, and mitigation of common risks, precise prediction of TBM PR holds significant importance. This study provided two hybrid prediction models based on XGBoost optimized by SSA and WOA alongside four ML models, including XGBoost, RF, SVM, and ANN, which served as benchmarks based on a database created in Shenzhen, China. Compared to empirical and theoretical models, the proposed hybrid XGBoost model incorporates a more extensive set of variables, and it does not rely on constants that might limit its applicability. When compared to previously reported machine learning models in previous studies, the hybrid XGBoost model demonstrates superior prediction performance. However, in line with the well-known “no free lunch theorem,” no single algorithm outperforms all others when addressing all engineering problems. Therefore, the development of SSA-XGBoost and WOA-XGBoost models is significant. While the prediction model in this study was developed based on the TBM database from Shenzhen, the model framework and analysis methods can serve as a reference for similar engineering projects. For instance, in the prediction of TBM PR in other engineering sites, similar model development and evaluation processes can be applied. This approach enables the reliable prediction of TBM PR, effectively guiding metro construction projects.

6. Conclusions

Utilizing supervised learning techniques and swarm optimization algorithms, this study introduces two hybrid evolutionary models for TBM PR prediction. The primary findings of this research can be summarized as follows:

- (1) The use of a swarm intelligence algorithm (SSA and WOA) can effectively improve the XGBoost model’s performance.
- (2) The WOA-XGBoost model stands out as the most accurate predictor of TBM performance, and this model exhibits a potential for addressing other prediction challenges.
- (3) The CS emerges as the most influential parameter affecting the TBM performance.

Author Contributions: Conceptualization, Z.Y.; methodology, Z.Y. and C.L.; software, Z.Y.; validation, Z.Y., C.L. and J.Z.; formal analysis, Z.Y.; investigation, Z.Y.; resources, Z.Y., C.L. and J.Z.; data curation, Z.Y. and C.L.; writing—original draft preparation, Z.Y.; writing—review and editing, Z.Y.; visualization, Z.Y.; supervision, C.L.; project administration, J.Z. All authors have read and agreed to the published version of the manuscript.

Funding: This research received no external funding.

Data Availability Statement: The data presented in this study are openly available in the study of Yang et al. at [10.1007/s00366-020-01217-2], reference number [5].

Conflicts of Interest: The authors declare no conflict of interest.

References

1. Liu, Q.; Huang, X.; Gong, Q.; Du, L.; Pan, Y.; Liu, J. Application and Development of Hard Rock TBM and Its Prospect in China. *Tunn. Undergr. Space Technol.* **2016**, *57*, 33–46. <https://doi.org/10.1016/j.tust.2016.01.034>.
2. Zhang, Y.; Wei, M.; Su, G.; Li, Y.; Zeng, J.; Deng, X. A Novel Intelligent Method for Predicting the Penetration Rate of the Tunnel Boring Machine in Rocks. *Math. Probl. Eng.* **2020**, *2020*, 3268694. <https://doi.org/10.1155/2020/3268694>.
3. Jahed Armaghani, D.; Faradonbeh, R.S.; Momeni, E.; Fahimifar, A.; Tahir, M.M. Performance Prediction of Tunnel Boring Machine through Developing a Gene Expression Programming Equation. *Eng. Comput.* **2018**, *34*, 129–141. <https://doi.org/10.1007/s00366-017-0526-x>.
4. Harandizadeh, H.; Armaghani, D.J.; Asteris, P.G.; Gandomi, A.H. *TBM Performance Prediction Developing a Hybrid ANFIS-PNN Predictive Model Optimized by Imperialism Competitive Algorithm*; Springer: London, UK, 2021; Volume 33, ISBN 0052102106.
5. Torabi, S.R.; Shirazi, H.; Hajali, H.; Monjezi, M. Study of the Influence of Geotechnical Parameters on the TBM Performance in Tehran-Shomal Highway Project Using ANN and SPSS. *Arab. J. Geosci.* **2013**, *6*, 1215–1227. <https://doi.org/10.1007/s12517-011-0415-3>.

6. Zeng, J.; Roy, B.; Kumar, D.; Mohammed, A.S.; Armaghani, D.J.; Zhou, J.; Mohamad, E.T. Proposing Several Hybrid PSO-Extreme Learning Machine Techniques to Predict TBM Performance. *Eng. Comput.* **2021**, *38*, 1–17. <https://doi.org/10.1007/s00366-020-01225-2>.
7. Hassanpour, J.; Ghaedi Vanani, A.A.; Rostami, J.; Cheshomi, A. Evaluation of Common TBM Performance Prediction Models Based on Field Data from the Second Lot of Zagros Water Conveyance Tunnel (ZWCT2). *Tunn. Undergr. Space Technol.* **2016**, *52*, 147–156. <https://doi.org/10.1016/j.tust.2015.12.006>.
8. Shan, F.; He, X.; Jahed Armaghani, D.; Zhang, P.; Sheng, D. Success and Challenges in Predicting TBM Penetration Rate Using Recurrent Neural Networks. *Tunn. Undergr. Space Technol.* **2022**, *130*, 104728. <https://doi.org/10.1016/j.tust.2022.104728>.
9. Yang, H.; Wang, Z.; Song, K. A New Hybrid Grey Wolf Optimizer-Feature Weighted-Multiple Kernel-Support Vector Regression Technique to Predict TBM Performance. *Eng. Comput.* **2022**, *38*, 2469–2485. <https://doi.org/10.1007/s00366-020-01217-2>.
10. Rostami, J. *Development of a Force Estimation Model for Rock Fragmentation with Disc Cutters through Theoretical Modeling and Physical Measurement of Crushed Zone Pressure*; Colorado School of Mines: Golden, CO, USA, 1997.
11. Bruland, A. *Hard Rock Tunnel Boring*; Norwegian University of Science and Technology: Trondheim, Norway, 1998.
12. Koopialipoor, M.; Nikouei, S.S.; Marto, A.; Fahimifar, A.; Jahed Armaghani, D.; Mohamad, E.T. Predicting Tunnel Boring Machine Performance through a New Model Based on the Group Method of Data Handling. *Bull. Eng. Geol. Environ.* **2019**, *78*, 3799–3813. <https://doi.org/10.1007/s10064-018-1349-8>.
13. Alsaihati, A.; Elkatatny, S.; Gamal, H. Rate of Penetration Prediction While Drilling Vertical Complex Lithology Using an Ensemble Learning Model. *J. Pet. Sci. Eng.* **2022**, *208*, 109335. <https://doi.org/10.1016/j.petrol.2021.109335>.
14. Mohapatra, P.; Chakravarty, S.; Dash, P.K. An Improved Cuckoo Search Based Extreme Learning Machine for Medical Data Classification. *Swarm Evol. Comput.* **2015**, *24*, 25–49. <https://doi.org/10.1016/j.swevo.2015.05.003>.
15. Nhu, V.H.; Janizadeh, S.; Avand, M.; Chen, W.; Farzin, M.; Omidvar, E.; Shirzadi, A.; Shahabi, H.; Clague, J.J.; Jaafari, A.; et al. GIS-Based Gully Erosion Susceptibility Mapping: A Comparison of Computational Ensemble Data Mining Models. *Appl. Sci.* **2020**, *10*, 2039. <https://doi.org/10.3390/app10062039>.
16. Chen, Y.; Zhang, T.; Zhao, W.; Luo, Z.; Lin, H. Rotating Machinery Fault Diagnosis Based on Improved Multiscale Amplitude-Aware Permutation Entropy and Multiclass Relevance Vector Machine. *Sensors* **2019**, *19*, 4542. <https://doi.org/10.3390/s19204542>.
17. Qiu, Y.; Zhou, J. Short-Term Rockburst Damage Assessment in Burst-Prone Mines: An Explainable XGBOOST Hybrid Model with SCSO Algorithm. *Rock Mech. Rock Eng.* **2023**, 1–26. <https://doi.org/10.1007/s00603-023-03522-w>.
18. Zhou, J.; Shen, X.; Qiu, Y.; Shi, X.; Khandelwal, M. Cross-Correlation Stacking-Based Microseismic Source Location Using Three Metaheuristic Optimization Algorithms. *Tunn. Undergr. Space Technol.* **2022**, *126*, 104570. <https://doi.org/10.1016/j.tust.2022.104570>.
19. Li, C.; Zhou, J.; Du, K.; Armaghani, D.J.; Huang, S. Prediction of Flyrock Distance in Surface Mining Using a Novel Hybrid Model of Harris Hawks Optimization with Multi-Strategies-Based Support Vector Regression. *Nat. Resour. Res.* **2023**, 1–29. <https://doi.org/10.1007/s11053-023-10259-4>.
20. Shahani, N.M.; Zheng, X.; Liu, C.; Li, P.; Hassan, F.U. Application of Soft Computing Methods to Estimate Uniaxial Compressive Strength and Elastic Modulus of Soft Sedimentary Rocks. *Arab. J. Geosci.* **2022**, *15*, 384. <https://doi.org/10.1007/s12517-022-09671-6>.
21. Balaji, K.; Rabiei, M. Status of Data-Driven Methods and Their Applications in Oil and Gas Industry, Introduction to Data Driven Methods. In *SPE Europec Featured at 80th EAGE Conference and Exhibition*; OnePetro: Richardson, TX, USA, 2018; pp. 11–14.
22. Armaghani, D.J.; Mohamad, E.T.; Narayanasamy, M.S.; Narita, N.; Yagiz, S. Development of Hybrid Intelligent Models for Predicting TBM Penetration Rate in Hard Rock Condition. *Tunn. Undergr. Space Technol.* **2017**, *63*, 29–43. <https://doi.org/10.1016/j.tust.2016.12.009>.
23. Alvarez Grima, M.; Bruines, P.A.; Verhoef, P.N.W. Modeling Tunnel Boring Machine Performance by Neuro-Fuzzy Methods. *Tunn. Undergr. Space Technol.* **2000**, *15*, 259–269. [https://doi.org/10.1016/S0886-7798\(00\)00055-9](https://doi.org/10.1016/S0886-7798(00)00055-9).
24. Mahdevari, S.; Shahriar, K.; Yagiz, S.; Akbarpour Shirazi, M. A Support Vector Regression Model for Predicting Tunnel Boring Machine Penetration Rates. *Int. J. Rock Mech. Min. Sci.* **2014**, *72*, 214–229. <https://doi.org/10.1016/j.ijrmm.2014.09.012>.
25. Koopialipoor, M.; Tootoonchi, H.; Jahed Armaghani, D.; Tonnizam Mohamad, E.; Hedayat, A. Application of Deep Neural Networks in Predicting the Penetration Rate of Tunnel Boring Machines. *Bull. Eng. Geol. Environ.* **2019**, *78*, 6347–6360. <https://doi.org/10.1007/s10064-019-01538-7>.
26. Xu, H.; Zhou, J.; Asteris, P.G.; Armaghani, D.J.; Tahir, M.M. Supervised Machine Learning Techniques to the Prediction of Tunnel Boring Machine Penetration Rate. *Appl. Sci.* **2019**, *9*, 3715. <https://doi.org/10.3390/app9183715>.
27. Zhou, J.; Qiu, Y.; Armaghani, D.J.; Zhang, W.; Li, C.; Zhu, S.; Tarinejad, R. Predicting TBM Penetration Rate in Hard Rock Condition: A Comparative Study among Six XGB-Based Metaheuristic Techniques. *Geosci. Front.* **2021**, *12*, 101091. <https://doi.org/10.1016/j.gsf.2020.09.020>.
28. Wang, Y.; Gao, X.; Jiang, P.; Guo, X.; Wang, R.; Guan, Z.; Chen, L.; Xu, C. An Extreme Gradient Boosting Technique to Estimate TBM Penetration Rate and Prediction Platform. *Bull. Eng. Geol. Environ.* **2022**, *81*, 1–19. <https://doi.org/10.1007/s10064-021-02527-5>.

29. Agrawal, A.K.; Murthy, V.M.S.R.; Chattopadhyaya, S.; Raina, A.K. Prediction of TBM Disc Cutter Wear and Penetration Rate in Tunneling Through Hard and Abrasive Rock Using Multi-Layer Shallow Neural Network and Response Surface Methods. *Rock Mech. Rock Eng.* **2022**, *55*, 3489–3506. <https://doi.org/10.1007/s00603-022-02834-7>.
30. Yagiz, S.; Gokceoglu, C.; Sezer, E.; Iplikci, S. Application of Two Non-Linear Prediction Tools to the Estimation of Tunnel Boring Machine Performance. *Eng. Appl. Artif. Intell.* **2009**, *22*, 808–814. <https://doi.org/10.1016/j.engappai.2009.03.007>.
31. Song, K.; Yang, H.; Wang, Z. A Hybrid Stacking Framework Optimized Method for TBM Performance Prediction. *Bull. Eng. Geol. Environ.* **2023**, *82*, 27. <https://doi.org/10.1007/s10064-022-03047-6>.
32. Yang, H.; Liu, X.; Song, K. A Novel Gradient Boosting Regression Tree Technique Optimized by Improved Sparrow Search Algorithm for Predicting TBM Penetration Rate. *Arab. J. Geosci.* **2022**, *15*, 461. <https://doi.org/10.1007/s12517-022-09665-4>.
33. Chen, T.; He, T. Xgboost: Extreme Gradient Boosting. *R Package Version 0.4-2* **2015**, *1*, 1–4.
34. Friedman, J.H. Greedy Function Approximation: A Gradient Boosting Machine. *Ann. Stat.* **2001**, *29*, 1189–1232.
35. Zhou, J.; Qiu, Y.; Zhu, S.; Armaghani, D.J.; Khandelwal, M.; Mohamad, E.T. Estimation of the TBM Advance Rate under Hard Rock Conditions Using XGBoost and Bayesian Optimization. *Undergr. Space* **2021**, *6*, 506–515. <https://doi.org/10.1016/j.undsp.2020.05.008>.
36. Barnard, C.J.; Sibly, R.M. Producers and Scroungers: A General Model and Its Application to Captive Flocks of House Sparrows. *Anim. Behav.* **1981**, *29*, 543–550. [https://doi.org/10.1016/S0003-3472\(81\)80117-0](https://doi.org/10.1016/S0003-3472(81)80117-0).
37. Xue, J.; Shen, B. A Novel Swarm Intelligence Optimization Approach: Sparrow Search Algorithm. *Syst. Sci. Control Eng.* **2020**, *8*, 22–34. <https://doi.org/10.1080/21642583.2019.1708830>.
38. Mirjalili, S.; Lewis, A. The Whale Optimization Algorithm. *Adv. Eng. Softw.* **2016**, *95*, 51–67. <https://doi.org/10.1016/j.advengsoft.2016.01.008>.
39. Shahani, N.M.; Zheng, X.; Guo, X.; Wei, X. Machine Learning-Based Intelligent Prediction of Elastic Modulus of Rocks at Thar Coalfield. *Sustainability* **2022**, *14*, 3689. <https://doi.org/10.3390/su14063689>.
40. Wei, X.; Shahani, N.M.; Zheng, X. Predictive Modeling of the Uniaxial Compressive Strength of Rocks Using an Artificial Neural Network Approach. *Mathematics* **2023**, *11*, 1650. <https://doi.org/10.3390/math11071650>.
41. Li, E.; Yang, F.; Ren, M.; Zhang, X.; Zhou, J.; Khandelwal, M. Prediction of Blasting Mean Fragment Size Using Support Vector Regression Combined with Five Optimization Algorithms. *J. Rock Mech. Geotech. Eng.* **2021**, *13*, 1380–1397. <https://doi.org/10.1016/j.jrmge.2021.07.013>.
42. Hasanipanah, M.; Jahed Armaghani, D.; Bakhshandeh Amnieh, H.; Koopialipoor, M.; Arab, H. A Risk-Based Technique to Analyze Flyrock Results Through Rock Engineering System. *Geotech. Geol. Eng.* **2018**, *36*, 2247–2260. <https://doi.org/10.1007/s10706-018-0459-1>.
43. Barzegar, R.; Sattarpour, M.; Deo, R.; Fijani, E.; Adamowski, J. An Ensemble Tree-Based Machine Learning Model for Predicting the Uniaxial Compressive Strength of Travertine Rocks. *Neural Comput. Appl.* **2020**, *32*, 9065–9080. <https://doi.org/10.1007/s00521-019-04418-z>.
44. Ly, H.B.; Pham, B.T.; Le, L.M.; Le, T.T.; Le, V.M.; Asteris, P.G. Estimation of Axial Load-Carrying Capacity of Concrete-Filled Steel Tubes Using Surrogate Models. *Neural Comput. Appl.* **2021**, *33*, 3437–3458. <https://doi.org/10.1007/s00521-020-05214-w>.
45. Yu, Z.; Shi, X.; Zhou, J.; Gou, Y.; Rao, D.; Huo, X. Machine-Learning-Aided Determination of Post-Blast Ore Boundary for Controlling Ore Loss and Dilution. *Nat. Resour. Res.* **2021**, *30*, 4063–4078. <https://doi.org/10.1007/s11053-021-09914-5>.
46. Nguyen, H.; Bui, X.N.; Choi, Y.; Lee, C.W.; Armaghani, D.J. A Novel Combination of Whale Optimization Algorithm and Support Vector Machine with Different Kernel Functions for Prediction of Blasting-Induced Fly-Rock in Quarry Mines. *Nat. Resour. Res.* **2021**, *30*, 191–207. <https://doi.org/10.1007/s11053-020-09710-7>.
47. Hasanipanah, M.; Keshtegar, B.; Thai, D.K.; Troung, N.T. An ANN-Adaptive Dynamical Harmony Search Algorithm to Approximate the Flyrock Resulting from Blasting. *Eng. Comput.* **2022**, *38*, 1257–1269. <https://doi.org/10.1007/s00366-020-01105-9>.
48. Nguyen, H.; Bui, X.N. Soft Computing Models for Predicting Blast-Induced Air over-Pressure: A Novel Artificial Intelligence Approach. *Appl. Soft Comput. J.* **2020**, *92*, 106292. <https://doi.org/10.1016/j.asoc.2020.106292>.
49. Zhou, J.; Guo, H.; Koopialipoor, M.; Jahed Armaghani, D.; Tahir, M.M. Investigating the Effective Parameters on the Risk Levels of Rockburst Phenomena by Developing a Hybrid Heuristic Algorithm. *Eng. Comput.* **2021**, *37*, 1679–1694. <https://doi.org/10.1007/s00366-019-00908-9>.
50. Faradonbeh, R.S.; Armaghani, D.J.; Amnieh, H.B.; Mohamad, E.T. Prediction and Minimization of Blast-Induced Flyrock Using Gene Expression Programming and Firefly Algorithm. *Neural Comput. Appl.* **2018**, *29*, 269–281. <https://doi.org/10.1007/s00521-016-2537-8>.
51. Zorlu, K.; Gokceoglu, C.; Ocakoglu, F.; Nefeslioglu, H.A.; Acikalin, S. Prediction of Uniaxial Compressive Strength of Sandstones Using Petrography-Based Models. *Eng. Geol.* **2008**, *96*, 141–158. <https://doi.org/10.1016/j.enggeo.2007.10.009>.
52. Taylor, K.E. Summarizing Multiple Aspects of Model Performance in a Single Diagram. *J. Geophys. Res. Atmos.* **2001**, *106*, 7183–7192. <https://doi.org/10.1029/2000JD900719>.
53. Yang, Y.; Zhang, Q. A Hierarchical Analysis for Rock Engineering Using Artificial Neural Networks. *Rock Mech. Rock Eng.* **1997**, *30*, 207–222. <https://doi.org/10.1007/BF01045717>.

54. Li, E.; Zhou, J.; Shi, X.; Jahed Armaghani, D.; Yu, Z.; Chen, X.; Huang, P. Developing a Hybrid Model of Salp Swarm Algorithm-Based Support Vector Machine to Predict the Strength of Fiber-Reinforced Cemented Paste Backfill. *Eng. Comput.* **2021**, *37*, 3519–3540. <https://doi.org/10.1007/s00366-020-01014-x>.
55. Shahani, N.M.; Ullah, B.; Shah, K.S.; Hassan, F.U.; Ali, R.; Elkotb, M.A.; Ghoneim, M.E.; Tag-Eldin, E.M. Predicting Angle of Internal Friction and Cohesion of Rocks Based on Machine Learning Algorithms. *Mathematics* **2022**, *10*, 3875. <https://doi.org/10.3390/math10203875>.

Disclaimer/Publisher’s Note: The statements, opinions and data contained in all publications are solely those of the individual author(s) and contributor(s) and not of MDPI and/or the editor(s). MDPI and/or the editor(s) disclaim responsibility for any injury to people or property resulting from any ideas, methods, instructions or products referred to in the content.